The Journal of Adhesion

Effect of Grit-Blasting on the Surface Energy of Graphite/Epoxy Composites

F. J. Boerio[a]; B. Roby[a]; R. G. Dillingham[a]; R. H. Bossi[b]; R. L. Crane[c]

[a] Department of Chemical and Materials Engineering, University of Cincinnati, Cincinnati, Ohio, USA
[b] Boeing, Seattle, Washington, USA [c] Materials Directorate, Air Force Research Laboratory, Wright Patterson Air Force Base, Ohio, USA

PLEASE SCROLL DOWN FOR ARTICLE

Taylor & Francis
Taylor & Francis Group

Effect of Grit-Blasting on the Surface Energy of Graphite/Epoxy Composites

F. J. Boerio
B. Roby
R. G. Dillingham
Department of Chemical and Materials Engineering, University of
Cincinnati, Cincinnati, Ohio, USA

R. H. Bossi
Boeing, Seattle, Washington, USA

R. L. Crane
Materials Directorate, Air Force Research Laboratory,
Wright Patterson Air Force Base, Ohio, USA

Contact-angle measurements were used to determine the surface energies of graphite/epoxy composites before and after grit-blasting with 80- and 220-grit garnet particles. Two different composite systems cured at 350°F were considered but they behaved similarly. Contact angles made by a series of liquids, including water, ethylene glycol, glycerol, formamide, and methylene iodide on as-tooled and grit-blasted composite panels were measured using a contact-angle goniometer. The contact angles were used to determine the dispersive and polar components of the surface energy (γ_s^d, γ_s^p). However, instead of using the contact angles made by two liquids to determine the two components of the surface energy, we used the contact angles made by several liquids and a graphical technique to determine γ_s^d and γ_s^p and to improve the accuracy of the measurements. It was found that the surface energies of as-tooled composites were approximately $35\,mJ/m^2$ and were mostly dispersive; the polar components were small. After grit-blasting with 80- or 220-grit garnet, the dispersive component of the surface energy decreased somewhat whereas the polar component increased significantly; the total surface energy after grit-blasting with 80- or 220-grit garnet was approximately $50\,mJ/m^2$. Etching composites in oxygen plasmas had a similar effect on the dispersive and polar components of the surface energy and on the total surface energy. Grit-blasting with 220-grit alumina resulted in higher dispersive components of surface energy and lower polar components than grit-blasting with 220-grit garnet

19

even though the total surface energy was similar after grit-blasting with 220-grit garnet and alumina. Correcting the measured surface energies for the effects of roughness resulted in small decreases in the total surface energy of the grit-blasted composites. However, even after correcting for roughness, the surface energies of the grit-blasted composites were still significantly greater than those of the as-tooled composites, indicating that grit-blasting resulted in changes in surface chemistry as well as changes in surface morphology of the composites. These changes in surface chemistry certainly included the removal of mold release agents from the as-tooled composites but probably also involved the creation of free radicals and their reaction with atmospheric oxygen to introduce oxygen-containing functional groups on the surfaces of the composites.

1. INTRODUCTION

Composites consisting of polymer matrices reinforced with graphite fibers are attractive materials for structural applications in the aerospace industry because they are light in weight and have a high strength-to-weight ratio. Adhesive bonding is the preferred method for joining composites because it eliminates the need for cutting holes in the composites that would damage load-bearing fibers, eliminates the stress concentrations that would be associated with mechanical fasteners, and enables stresses to be distributed over large areas. In addition, adhesively bonded structures frequently have lower weight than similar structures that are assembled using mechanical fasteners.

Adhesives used for joining composites fall into two broad classes: high-temperature curing film adhesives and room-temperature curing paste adhesives. Although high-temperature curing film adhesives are less sensitive to composite surface preparation than room-temperature curing paste adhesives, the surface-preparation procedure is always critical to achieving a strong bond. Composite surfaces are frequently contaminated with release agents that are used to prevent adhesion of the composites to the molds in which they are cured. The presence of a release agent on the surface lowers the surface energy of a composite and makes it difficult for the room-temperature cure systems to wet the surface. As a result, surface engineering processes must frequently be applied to polymer composites to remove mold release agents from their surfaces and to increase their surface energies. These surface engineering processes may be as simple as rinsing the surface with a solvent. However, they may be much more complex, removing

release agents, roughening the surface to introduce topographical features that allow for mechanical interlocking between an adhesive and the surface, and changing the surface chemistry of the composites by introducing new functional groups.

Grit-blasting is a surface engineering process that is frequently applied to polymer composites. However, relatively little information is available concerning the effect of grit-blasting on the surface properties of composites. Chin and Wightman [1] considered the effect of several surface engineering processes, including grit-blasting, on the composition, surface energy, and surface topography of composites consisting of a toughened bismaleimide resin reinforced with carbon fibers. They found that the surfaces of the as-received composites consisted of approximately 12 atomic percent fluorine from residual mold-release agents. Grit-blasting with 150-grit silica particles at 414 kPa effectively removed the mold-release agents and increased the total surface energy of the composites. Before grit-blasting, the dispersive and polar components of the surface energy were 25.0 and $6.3 \, mJ/m^2$, respectively, and the total surface energy was $31.3 \, mJ/m^2$. After grit-blasting, the dispersive and polar components increased to 30.8 and $8.3 \, mJ/m^2$, respectively, and the total was $39.1 \, mJ/m^2$.

Chin and Wightman [1] also considered the effect of etching in an oxygen plasma on the surface properties of the bismaleimide composites. After plasma etching for 5 min, there was no detectable fluorine on the surfaces of the composites; the dispersive and polar components of the surface energy were 36.4 and $42.3 \, mJ/m^2$, respectively, and the total surface energy was $78.7 \, mJ/m^2$.

Finally, Chin and Wightman [1] reported that grit-blasting had a significant effect on the surface roughness of the composites. Surface roughness was expressed in terms of the roughness correction factor (R_c) that Wenzel [2] defined as the ratio of the actual area of a roughened surface to the projected area of the surface or as the ratio of the contact angles that a given liquid made on roughened and smooth surfaces. Chin and Wightman found that R_c increased from 1.03 ± 0.08 for the as-received composites to 1.33 ± 0.14 and 1.21 ± 0.12 for the grit-blasted and plasma-etched composites, respectively.

Pocius and Wenz [3] considered the effect of several surface engineering processes, including peel ply, grit-blasting with 100-grit alumina, sanding with 150-grit SiC abrasive paper mounted on an orbital sander, and abrasive treatment with a Scotchbrite® pad, on the surface composition and properties of graphite/epoxy composites. X-ray photoelectron spectrocopy (XPS) showed that the untreated composites had about 14.8% fluorine on their surfaces from residual mold-release agents but that the fluorine concentration was decreased

to 2.6% by grit-blasting, 0.4% by sanding, and to 1.2% after abrasion of the surface with a Scotchbrite 7446 pad. The dispersive and polar components of the surface energy of the untreated composites were 32 and $4 \, \text{mJ/m}^2$, respectively. After grit-blasting, the dispersive and polar components of the surface energy were 33 and $11 \, \text{mJ/m}^2$, respectively; grit-blasting, thus, primarily affected the polar component of surface energy. Sanding and abrasion with the Scotchbrite pad had somewhat smaller effects on the surface energies of the composites. Thus, after sanding, the dispersive and polar components of surface energy were 37 and $4 \, \text{mJ/m}^2$, respectively. After abrasion with the Scotchbrite pad, the dispersive and polar components of surface energy were 35 and $6 \, \text{mJ/m}^2$, respectively.

Harris and Beevers investigated the surface properties of aluminum and steel that were grit-blasted with alumina [4]. They also expressed the total surface energy as the sum of dispersive and polar components and found that grit-blasted surfaces had higher surface energies than solvent-wiped surfaces and that coarser grits produced rougher surfaces with lower surface energies than finer grits.

Despite the importance of epoxy matrix composites, there have been few published reports concerning the effect of grit-blasting on their surface properties. The objective of this article is to describe the effect of grit-blasting and plasma etching on the surface energy and surface roughness of epoxy matrix composites reinforced with graphite fibers. Subsequent papers will discuss the effects of grit-blasting and plasma etching on the surface composition of the composites and on the characteristics of adhesive joints prepared from grit-blasted and plasma-etched composites.

2. BACKGROUND

2.1. Surface Energies of Composites

Most discussions concerned with the surface energy of materials begin with the Young equation

$$\gamma_{sv} = \gamma_s - \pi_s = \gamma_{lv} \cos(\theta) + \gamma_{sl} \tag{1}$$

in which θ is the contact angle that a liquid makes with the surface of a solid substrate, γ_{sv} is the surface energy of the substrate in equilibrium with the vapor of the liquid, γ_s is the true surface energy of the substrate, π_s is the equilibrium spreading pressure of the liquid on the solid, γ_{lv} is the surface energy of the liquid, and γ_{sl} is the interfacial energy of the liquid and solid.

γ_{lv}, the surface energy of the liquid, is usually known whereas θ is measured experimentally. To determine γ_{sv}, the surface energy of the solid, it is necessary to know γ_{sl}. Although several expressions have been proposed for γ_{sl}, we have used the expression suggested by Kaelble and Uy [5]:

$$\gamma_{sl} = \gamma_s + \gamma_{lv} - 2(\gamma_s^d \gamma_{lv}^d)^{1/2} - 2(\gamma_s^p \gamma_{lv}^p)^{1/2}. \tag{2}$$

This expression assumes that the surface energies of the liquid and solid can be separated into contributions from "dispersion" and "polar" forces and that the interfacial energy of the liquid and the substrate can be expressed as the geometrical mean. Chin and Wightman [1] and Harris and Beevers [4] used the same approach.

When Equation (2) is substituted into the Young equation, the result shown in Equation (3) is obtained. Equation (3) relates the contact angle of a liquid on a solid to the dispersive and polar components of the surface energies of the liquid and the solid:

$$\cos(\theta) = -1 + \frac{[2(\gamma_s^d \gamma_{lv}^d)^{1/2} + 2(\gamma_s^p \gamma_{lv}^p)^{1/2} - \pi_s]}{\gamma_{lv}}. \tag{3}$$

If the contact angle for a liquid with surface energy $\gamma_{lv} = \gamma_{lv}^d + \gamma_{lv}^p$ is measured, then the contact angle can be substituted into Equation (3) along with the corresponding values of $\gamma_{lv}, \gamma_{lv}^d$, and γ_{lv}^p. This provides one equation with two unknowns, γ_s^d and γ_s^p (π_s is usually taken to be zero for low-energy surfaces such as those considered here). To determine the two unknowns, γ_s^d and γ_s^p, it is necessary to measure the contact angle made by a second liquid and to substitute the measured value into Equation (3) along with the appropriate values of $\gamma_{lv}, \gamma_{lv}^d$, and γ_{lv}^p. This provides two equations with two unknowns, γ_s^d and γ_s^p; these equations can be solved simultaneously for γ_s^d and γ_s^p.

Although this "two-liquid" method for determining the dispersive and polar components of the surface energy of a solid is useful, it is very desirable to use the measured contact angles of several liquids, not just two, to improve the accuracy with which γ_s^d and γ_s^p are determined. To do this, Equation (3) can be rearranged as shown:

$$\gamma_{lv} \frac{[1 + \cos(\theta)]}{2(\gamma_{lv}^p)^{1/2}} = (\gamma_s^d)^{1/2} \left(\frac{\gamma_{lv}^d}{\gamma_{lv}^p}\right)^{1/2} + (\gamma_s^p)^{1/2}. \tag{4}$$

This is the equation of a straight line. Thus, the contact angles made by any number of liquids can be measured and the parameter $\gamma_{lv}[1 + \cos(\theta)]/2(\gamma_{lv}^p)^{1/2}$ that appears on the left-hand side of Equation

(4) can be plotted against the parameter $(\gamma_{lv}^d / \gamma_{lv}^p)^{1/2}$ that appears on the right-hand side of the equation. The resulting plot should give a straight line; the slope of the line should equal $(\gamma_s^d)^{1/2}$ and the intercept equals $(\gamma_s^p)^{1/2}$. We refer to such plots as "linear Kaelble" plots.

2.2. Wettability Envelopes

The Young equation [Equation (1)] can be rearranged to

$$\frac{(\gamma_{sv} - \gamma_{sl})}{\gamma_{lv}} = \cos(\theta). \tag{5}$$

The cosine term on the right-hand side of Equation (5) can obviously never have a value that is greater than 1.0. However, the left-hand side of Equation (5) can have a value greater than 1.0. The condition for a liquid to just wet and spread across the surface of a substrate is that $\theta = 0.0$. Therefore, the condition for a liquid to just wet a surface and spread across it is that

$$\frac{(\gamma_{sv} - \gamma_{sl})}{\gamma_{lv}} \geq 1.0 \tag{6}$$

or that

$$(\gamma_{sv} - \gamma_{sl}) \geq \gamma_{lv}. \tag{7}$$

Assuming the form for γ_{sl} given in Equation (2) and rearranging, Equation (7) can be written as

$$(\gamma_s^d \gamma_{lv}^d)^{1/2} + (\gamma_s^p \gamma_{lv}^p)^{1/2} \geq \gamma_{lv}. \tag{8}$$

According to Equation (8), a liquid will wet and spread across the surface of a solid substrate if the left-hand side of the equation is equal to or greater than the right-hand side. The condition for wetting and spreading of the liquid to *just* occur is obtained by setting the left-hand side of Equation (8) equal to the right-hand side as shown in Equation (9):

$$(\gamma_s^d \gamma_{lv}^d)^{1/2} + (\gamma_s^p \gamma_{lv}^p)^{1/2} = \gamma_{lv} \tag{9}$$

If γ_s^d and γ_s^p are known for the surface of the solid, the values of γ_{lv}^d, γ_{lv}^p, and γ_{lv} that satisfy Equation (9) can be determined. A plot of γ_{lv}^d against γ_{lv}^p can then be constructed using the values of γ_{lv}^d and γ_{lv}^p that satisfy Equation (9). This plot will define a contour that is referred to as a "wettability envelope." Any liquid whose coordinates $(\gamma_{lv}^d, \gamma_{lv}^p)$ lie on the contour or within it will wet the surface but liquids having coordinates $(\gamma_{lv}^d, \gamma_{lv}^p)$ that lie outside the contour will not [6].

2.3. Roughness

As indicated, Wenzel [2] suggested that the contact angle that a liquid makes with the roughened surface of a solid is θ_r whereas the contact angle made by the same liquid in the absence of roughness is θ_o. He then defined a roughness factor R_c as

$$R_c = \frac{\cos(\theta_r)}{\cos(\theta_o)} = \frac{A_r}{A_o} \tag{10}$$

where A_r and A_o are the actual and projected areas of the surface. We used Wenzel's approach to correct measured contact angles for the effects of roughness by measuring the contact angles that two liquids, water and glycerol, made with smooth and grit-blasted glass substrates. The corrected values of the contact angles were obtained as

$$\theta_o = \cos^{-1}\left[\frac{\cos(\theta_r)}{R_c}\right] \tag{11}$$

However, to eliminate the effects of differences in surface chemistry caused by the roughening process, the smooth and roughened glass surfaces were coated with gold before the contact angles were determined as suggested by Carre and Schultz [7].

3. EXPERIMENTAL

Panels of two different composite systems consisting of epoxy resins reinforced with graphite fibers were prepared at Boeing. These composites, which are referred to as System 1 and System 2, were both cured at 177°C (350°F). Most of the panels were grit-blasted at Boeing using a robotic system and either 80- or 220-grit garnet particles (HPX grade, Barton Mines Company, Lake George, NY) and then sent to UC (The University of Cincinnati, Cincinnati, OH) where contact angles were measured. The garnet had a Knoop hardness of 1700–2000 and a specific gravity of 3.9–4.1. In a few cases, 220-grit alumina (Duralum Special White, Washington Mills, North Grafton, MA) was also used. This material had a Knoop hardness of 2000 and specific gravity of 3.96. The pressure used for grit-blasting was 621 kPa (90 psi), the distance from the nozzle to the sample was 11.43 cm (4.5 in.), and the raster rate was 12.7 cm/s (5 in./s). The composite panels were designated as R1–R8; their characteristics are summarized in Table 1.

In some cases, as-tooled composites were etched in oxygen plasmas at UC to remove mold-release agents and to insert oxygen-containing functional groups into their surfaces. Plasma etching was carried out

TABLE 1 Panel ID, Composite System, and Pretreatment for Panels R1-R8

Panel ID	Composite system	Pretreatment
Rl	1	As-tooled
R2	1	80-grit garnet
R3	1	220-grit garnet
R4	1	220-grit aluminum oxide
R5	2	As-tooled
R6	2	80-grit garnet
R7	2	220-grit garnet
R8	2	220-grit aluminum oxide

in a capacitively coupled, parallel-plate, radio-frequency (RF)-powered plasma reactor using a power of 50 W and a time of 30 s. The electrodes in this reactor were oriented horizontally and were spaced 3.0 cm apart. The upper electrode was powered and the lower electrode was grounded. Samples were placed on the lower electrode during plasma etching.

Contact angles made by various liquids with the composites were measured at UC using a Rame–Hart contact-angle goniometer after wiping the surfaces of the composites with ethanol. The surface energies of the liquids that were used to measure contact angles are summarized in Table 2; the surface energies of these liquids were obtained from the literature [8]. Not all of these liquids were used to determine the surface energy of each panel because in some cases, especially for grit-blasted or plasma-etched panels, some of the liquids completely wetted the surfaces of the panels. The advancing contact angles were measured by placing two droplets of each liquid onto the surface of a substrate using a glass microliter syringe. Sufficient time was allowed for the droplets to reach equilibrium and stop spreading. Then the contact angles that the left and right sides of each droplet made with the

TABLE 2 Dispersive and Polar Components of the Surface Energies of Liquids Used in Contact-Angle Measurements

Liquid	γ_{lv}^{d} (mJ/m^2)	γ_{lv}^{p} (mJ/m^2)	γ_{lv} (mJ/m^2)
Water	22.0	50.2	72.2
Glycerol	34.0	30.0	64.0
Di-iodomethane	48.5	2.3	50.8
Ethylene glycol	29.3	19.0	48.3
Dimethylsulfoxide	34.9	8.7	43.6
Formamide	32.3	26.0	58.3
Tricresylphosphate	36.2	4.5	40.7

substrate were measured and averaged. Thus, the contact angles were actually the average of four measurements.

The surface tension of the uncured paste adhesive Hysol EA-9396 (Henkel Corp., Bay Point, CA) was determined using the DuNuoy ring technique [9]. One hundred parts by weight of part A (epoxy-containing component) were mixed with 17 parts of part B (curing agent) at room temperature to prepare the adhesive. A platinum ring was immersed into the uncured adhesive and then slowly withdrawn. The force required to just detach the ring from the adhesive was determined and the surface tension of the uncured adhesive was calculated using the equation

$$F = 4\pi r\gamma \tag{12}$$

in which r is the radius of the ring, γ is the surface tension of the adhesive, and F is the force. Five determinations were averaged to get the final value of γ. Viscous effects were not considered because the ring was withdrawn from the uncured adhesive very slowly.

Because of difficulties in obtaining complete coverage and good adhesion of evaporated gold films to grit-blasted composite substrates, roughness factors were determined for grit-blasted glass substrates rather than composites even though significant differences were expected in hardness and brittleness between glass and the composites. Glass substrates were grit-blasted with 80- or 220-grit garnet at Boeing and sent to UC where thin films of gold were evaporated onto them. Similar but smooth glass substrates that were not grit-blasted were also coated with gold. Contact angles made by water and glycerol on gold-coated, smooth, and rough glass surfaces were measured, and roughness factors were determined using Equation (10). The measured contact angles were corrected for the effects of roughness using Equation (11).

4. RESULTS AND DISCUSSION

The surface tension of uncured EA-9396 was $39.0 \pm 0.8\,\mathrm{mJ/m^2}$. This value was similar to those obtained for other amine-cured epoxy adhesive systems. For example, Page and coworkers [10] used dynamic contact-angle analysis to obtain a value of $36.3\,\mathrm{mJ/m^2}$ for an adhesive consisting of a DGEBA epoxy resin and an isophorone diamine curing agent. Grundke [11] obtained a value of about $37.5\,\mathrm{mJ/m^2}$ for a similar adhesive system using axisymmetric drop shape analysis.

Roughness factors of 1.07 for glass that was grit-blasted with 220-grit garnet and approximately 1.13 for glass that was blasted with

TABLE 3 Roughness Factors for Glass that Was Grit-Blasted with 80- or 220-Grit Garnet and Then Coated with Gold by Evaporation

Grit	R_a (glycerol)	R_a (water)
80	1.11	1.16
220	1.07	1.07

80-grit garnet were obtained (see Table 3). As expected, the roughness factor was greater for the substrate that was grit-blasted with the 80-grit garnet. Contact angles made by a liquid placed on a composite panel that was grit-blasted were subsequently corrected for roughness by dividing $\cos(\theta_r)$ by the appropriate R_a value (1.07 for 220 grit or the average value of 1.13 for 80 grit) to get $\cos(\theta_o)$.

The contact angles made by a series of liquids were measured for panels R1–R8 at UC and used to construct linear Kaelble plots. Dispersive and polar components of the surface energy of each panel were determined from the slope and intercept of these plots. The uncertainty in the measured values of the contact angles was less than $\pm 0.4°$.

Examples of linear Kaelble plots are shown in Figures 1 (panel R1), 2 (panel R3), 3 (panel R4), and 4 (panel R5 after plasma etching). Error bars were not included in these figures because the errors in the data points were smaller than the markers used to locate the various data points. Reference to Figure 1 shows that the intercept of the linear
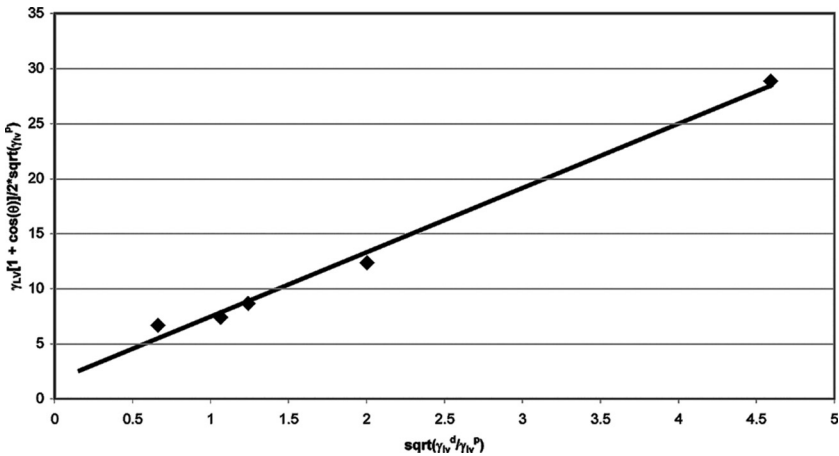
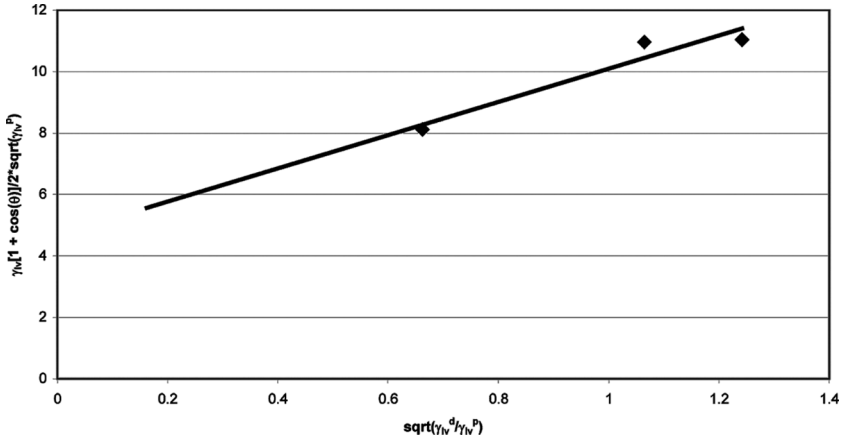**FIGURE 1** Linear Kaelble plot for as-tooled panel R1.

FIGURE 2 Linear Kaelble plot for panel R3. This panel was grit-blasted with 220-grit garnet.

Kaelble plot for panel R1 was small, indicating that the polar component of the surface energy of R1 was small. Small polar components were expected for as-tooled composites whose surfaces were probably contaminated by mold-release agents. Figures 2–4 show that the intercepts of the linear Kaelble plots for panels R3, R4, and R5 after plasma
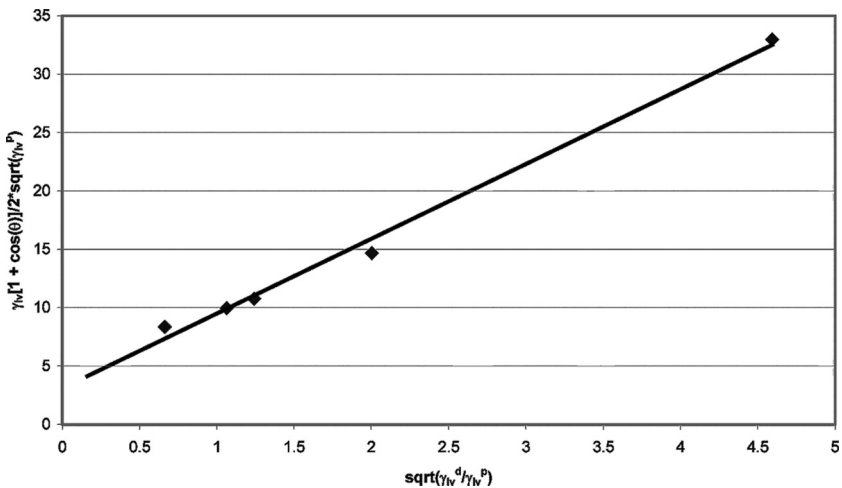

FIGURE 3 Linear Kaelble plot for panel R4. This panel was grit-blasted with 220-grit aluminum oxide.
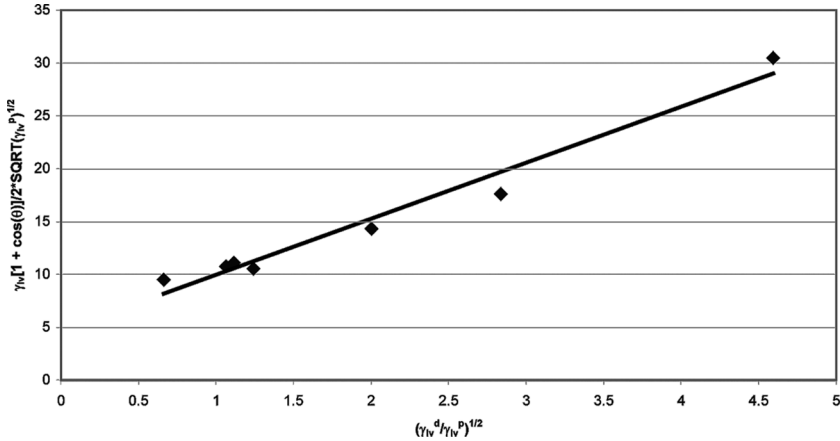
FIGURE 4 Linear Kaelble plot for panel R5. This panel was as-tooled but was etched in an O_2 plasma for 30 s.

etching were significantly greater, indicating that grit-blasting and plasma etching had significant effects on the polar components of the surface energy of the composites.

The surface energies of composite panels R1–R8 and panels R1 and R5 after plasma etching are shown in Table 4. These surface energies were determined from linear Kaelble plots and are expressed as the dispersive component followed by the polar component. Table 4 indicates that the surface energies of the as-tooled panels (R1 and R5) were about 36.7 ± 0.4 and $35.4 \pm 0.4\,\mathrm{mJ/m}^2$, respectively. The surface energies of all of the grit-blasted panels were significantly higher and were between about 45 and $51\,\mathrm{mJ/m}^2$. Surface energies of plasma-etched panels R1 and R5 were similar to those of grit-blasted panels and were 49.0 ± 0.4 and $49.9 \pm 0.4\,\mathrm{mJ/m}^2$, respectively. The changes in surface energy resulting from grit-blasting were not associated with residual grit-blasting media because little evidence for grit particles was obtained from surface analysis. A more complete discussion of this point will be given in a subsequent paper.

Grit-blasting with 80- and 220-grit garnet resulted in decreases of approximately $5\,\mathrm{mJ/m}^2$ in the dispersive component of the surface energies of the composites. However, grit-blasting with 80- and 220-grit garnet resulted in increases of approximately $20\,\mathrm{mJ/m}^2$ in the polar component of the surface energies of the composites. Grit-blasting seemed to have slightly different effects on panels of System 1 and System 2 composites. Thus, the decrease in the dispersive component of the surface energy and the increase in the polar component after

TABLE 4 Surface Energies of Composite Panels R1–R8 and Panels R1 and R5 after Plasma Etching

ID	System	Pretreatment	Surface energy, no Ra correction (mJ/m²)			Surface energy, after correction (mJ/m²)		
			γ_s^d	γ_s^p	γ_s	γ_s^d	γ_s^p	γ_s
R1	1	As-tooled	34.1 ± 0.3	2.6 ± 0.3	36.7 ± 0.4	—	N/A	—
R2	1	80-grit garnet	28.8 ± 0.7	20.0 ± 0.7	48.8 ± 1.0	23.6 ± 0.6	20.1 ± 0.6	43.7 ± 0.8
R3	1	220-grit garnet	29.2 ± 0.6	22.0 ± 0.6	51.2 ± 0.8	25.8 ± 0.5	20.0 ± 0.6	45.8 ± 0.8
R4	1	220-grit Al_2O_3	41.0 ± 0.2	9.6 ± 0.3	50.6 ± 0.4	—	N/A	—
R5	2	As-tooled	34.5 ± 0.4	0.9 ± 0.2	35.4 ± 0.4	—	N/A	—
R6	2	80-grit garnet	31.6 ± 0.9	14.5 ± 0.6	46.1 ± 1.1	25.8 ± 0.7	15.1 ± 0.6	40.9 ± 0.9
R7	2	220-grit garnet	30.6 ± 0.9	15.6 ± 0.7	46.2 ± 1.1	27.4 ± 0.8	15.9 ± 0.6	43.3 ± 1.0
R8	2	220-grit Al_2O_3	43.1 ± 0.3	1.2 ± 0.1	44.3 ± 0.3	—	N/A	—
R1	1	As-tooled + plasma	29.0 ± 0.2	20.1 ± 0.4	49.1 ± 0.4	—	N/A	—
R5	2	As-tooled + plasma	28.1 ± 0.2	21.8 ± 0.4	49.9 ± 0.4	—	N/A	—

Note: The surface energies were determined from linear Kaelble plots and are expressed as the dispersive component followed by the polar component.

31

grit-blasting with 80- and 220-grit garnet were greater for panels of System 1 composite than for panels of System 2 composite.

Grit-blasting with 220-grit alumina had a different effect on the surface energy of the composites than did grit-blasting with 220-grit garnet. Thus, grit-blasting with 220-grit alumina resulted in an increase of about $6\,\mathrm{mJ/m^2}$ in the dispersive component of the surface energy of System 1 panels and a similar increase in the polar component. In the case of System 2 composites, grit-blasting with 220-grit alumina increased the dispersive component of surface energy by approximately $9\,\mathrm{mJ/m^2}$ but had little effect on the polar component. Differences in surface energy after grit-blasting with 220-grit garnet and alumina were probably related to differences in the shape of the garnet and alumina particles.

An interesting aspect of the results shown in Table 4 is that correcting for roughness resulted in a small decrease in the surface energy of System 1 composites that were grit-blasted with 80- and 220-grit garnet. Most of this decrease was in the dispersive component of surface energy. However, even after correcting for roughness, the surface energies of the grit-blasted composites were still significantly larger than those of the as-tooled composites. This indicated that grit-blasting resulted in changes in the surface *composition* of the composites as well as changes in their *morphology*. Changes in the surface composition certainly arose from the removal of mold-release agents and other contaminants from the surfaces of the composites. However, other factors, such as the introduction of free radicals, may have affected the surface composition of the composites during grit-blasting.

Etching in an O_2 plasma for 30 s resulted in a large increase in the surface energy of R1, from 36.7 ± 0.4 to $49.1 \pm 0.4\,\mathrm{mJ/m^2}$ and in a similar increase in the surface energy of R5, from 35.4 ± 0.4 to $49.9 \pm 0.4\,\mathrm{mJ/m^2}$ (see Table 4). In fact, panels that were plasma etched had surface energies that were very similar to those of panels that were grit-blasted with 80- or 220-grit garnet. However, the surface energies of plasma-etched composites were greater than those of grit-blasted composites after the surface energies of the grit-blasted composites were corrected for roughness.

It was not possible to make specific comparisons between the results obtained here and those obtained by Chin and Wightman because the composite systems and the experimental procedures that they used were much different from those used here. Nevertheless, some general comparisons were made. They found that grit-blasting increased the total surface energy of graphite/bismaleimide composites; we found similar results for graphite/epoxy composites. However, Chin and Wightman found that grit-blasting resulted in larger

changes in the dispersive component of the surface energy than in the polar component; we found the opposite trend, with grit-blasting having a greater effect on the polar component of surface energy than on the dispersive component. They found that plasma etching increased the dispersive and polar components of the surface energy significantly whereas we found that plasma etching decreased the dispersive component somewhat and greatly increased the polar component.

The roughness correction factor that Chin and Wightman obtained for bismaleimide composites that were grit-blasted with 150-grit silica was 1.33 ± 0.14; we found values of approximately 1.07 and 1.13 for epoxy composites blasted with 220- and 80-grit garnet, respectively. The roughness correction factor that they obtained was obviously much greater than those obtained in our work. Perhaps the most significant difference between their work and ours was that they made three passes across a composite with the nozzle of the gun located about 15–20 cm from the panels. We made only a single pass across a panel with a nozzle that was 11.4 cm from the surface of the composite.

Similarly, it is difficult to compare our results with those of Pocius and Wenz because of the differences in materials and techniques that were used in their work and in ours. However, as shown in Table 4, the surface energies of the as-tooled composites used here ($\gamma_s^d = 34.1 \pm 0.3 \, \text{mJ/m}^2, \gamma_s^p = 2.6 \pm 0.3 \, \text{mJ/m}^2$ for System 1 panels; $\gamma_s^d = 34.5 \pm 0.4 \, \text{mJ/m}^2, \gamma_s^p = 0.9 \pm 0.2 \, \text{mJ/m}^2$ for System 2 panels) were very similar to those of their untreated composites ($\gamma_s^d = 32 \, \text{mJ/m}^2, \gamma_s^p = 4 \, \text{mJ/m}^2$). In addition, Pocius and Wenz found that grit-blasting with silica particles primarily affected the polar component of surface energy. In our work, it was found that grit-blasting with 80- and 220-grit garnet particles affected mostly the polar component of surface energy. However, grit-blasting with 220-grit alumina seemed to affect mostly the dispersive component.

Wettability envelopes for panels R1 and R2 with no roughness correction and R2 with roughness correction are shown in Figure 5. These wettability envelopes were calculated using values of γ_s^d and γ_s^p from Table 4. Data points for several liquids, including water, diiodomethane, dimethylsulfoxide, glycerol, and ethylene glycol are also shown in Figure 5. Similar wettability envelopes for panels R1 and R3 with no roughness correction and R3 with roughness correction are shown in Figure 6. It should be noted that the uncertainty in the surface energies of the composites would affect the wettability envelopes by expanding or contracting the envelopes by approximately $1.0 \, \text{mJ/m}^2$.
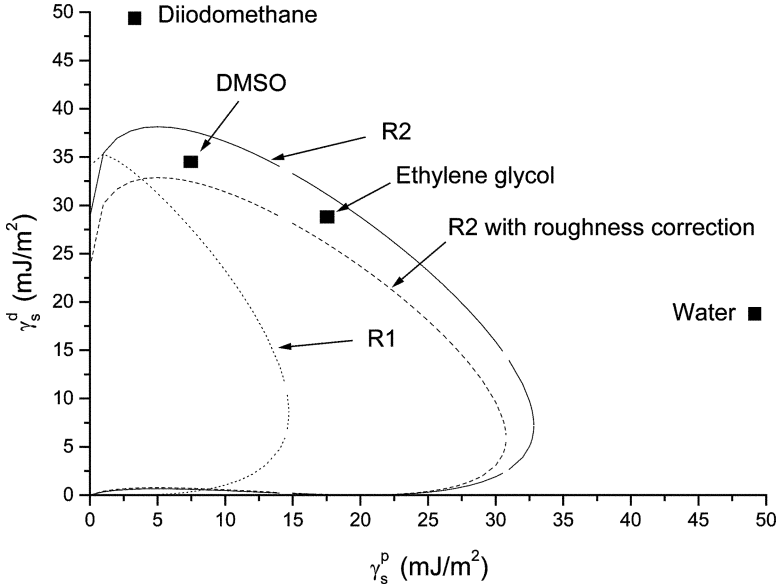
FIGURE 5 Wettability envelopes for panels R1 ($\cdots$), R2 with no roughness correction (——), and R2 with roughness correction ($----$).
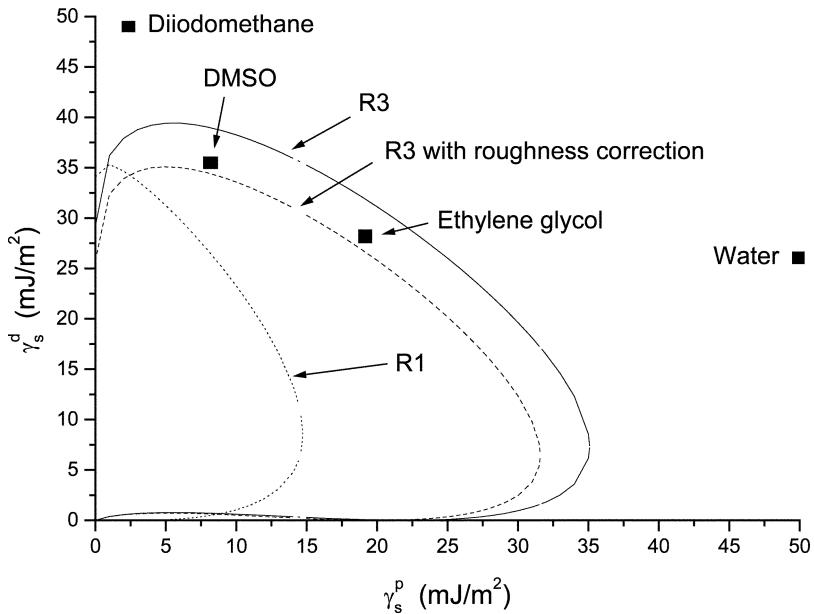

FIGURE 6 Wettability envelopes for panels R1 ($\cdots$), R3 with no roughness correction (—), and R3 with roughness correction ($----$).

There were several important aspects to these wettability envelopes. One was that the envelopes for grit-blasted composites encompassed much greater areas than those for as-tooled panels. This meant that the range of liquids, including adhesives, which would wet the grit-blasted substrates was much greater than the range of liquids that would wet the as-tooled substrates. Another interesting aspect of the wettability envelopes was that correcting for roughness resulted in only a small decrease in the encompassed area. This observation was consistent with the conclusion that grit-blasting caused a significant change in the surface chemistry of the composites as well as an increase in the roughness. The change in surface chemistry involved the removal of contaminants from the surface but it probably involved other effects, such as the formation of free radicals.

Numerous investigations have been reported regarding free-radical generation in polymers subjected to mechanical deformation. Electron spin resonance spectroscopy (ESR) has been employed to detect free-radical products. Fanconi et al. [12] investigated free-radical generation in linear and ultrahigh-molecular-weight polyethylene samples that were ground with a dental burr in a hand grinder. ESR studies of linear polyethylene showed that the concentration of free radicals was about 1.2×10^{16} at $-150°C$ and 1.0×10^{16} upon warming of the sample to $-50°C$. Ultrahigh-molecular-weight polyethylene showed free-radical concentrations of 10^{17} at $-150°C$ and upon warming to $-50°C$. These concentrations were in good agreement with the number of new end groups determined by Fourier-transform infrared spectroscopy.

Peterlin [13] investigated free-radical generation in polyethylene terephthalate (PET) fibers using electron paramagnetic resonance spectroscopy. It was shown that PET undergoes structural changes that are induced mechanically. During stretching, end-of-chain radicals formed that decayed to secondary center-of-chain radicals by mechanisms such as proton transfer.

Pace and Roland [14] investigated free-radical formation in PET fibers that were abraded in a ceramic container under liquid nitrogen using a power drill equipped with a metal or sandstone bit. EPR results indicated the formation of a benzoyloxy-type radical structure that formed through cleavage of the ester bond in the PET repeat unit. It seems likely that free radicals were formed during grit-blasting of the composites investigated here and that some of the radicals reacted with oxygen in the atmosphere to introduce oxygen-containing functional groups into the surface regions of the composites.

Another important aspect of the wettability envelopes was that the adhesive EA-9396 was expected to wet the grit-blasted composites but not the as-tooled composites. As indicated previously, the total surface

tension for uncured EA-9396 was about $39.0 \pm 0.8 \, \text{mJ/m}^2$. Although the dispersive and polar components of the surface tension of EA-9396 were not determined individually, the coordinates (γ_s^d, γ_s^p) for EA-9396 would lie inside the envelopes for R2 and R3 but outside the envelope for R1 for any reasonable values of the dispersive and polar components of the surface tension.

It can also be observed from Figures 5 and 6 that the coordinates for dimethylsulfoxide (DMSO) were inside the envelope for grit-blasted panels but outside the envelope for as-tooled composites. This indicated that DMSO should wet grit-blasted panels but not as-tooled panels. This result correlated well with experience at UC and at Boeing and showed that the wetting behavior of DMSO could be used to determine whether a composite panel was suitable for bonding.

5. SUMMARY

These results can be summarized by saying that grit-blasting increased the surface energy of graphite/epoxy composites as well as their surface roughness. Eighty-grit garnet had a greater effect on surface roughness than 220-grit garnet but both resulted in similar surface energies. The type of particles used in grit-blasting affected the surface energies of the composites. Thus, grit-blasting with 220-grit alumina resulted in different surface energies than did grit-blasting with 220-grit garnet. The nature of the composite also had an effect on surface energy after grit-blasting. Thus, panels of System 1 composites had a greater surface energy after grit-blasting than did panels of System 2 composites even though Systems 1 and 2 were both graphite/epoxy composites and both were cured at 177°C (350°F). After correcting for roughness, the surface energies of composites that were grit-blasted were greater than the surface energies of as-tooled composites, emphasizing that grit-blasting affected the surface composition of composites as well as their surface morphology. Composites that were etched in an O_2 plasma had surface energies that were similar to those of composites that were grit-blasted. However, after correcting for roughness, the surface energies of composites that were grit-blasted were smaller than those of panels that were plasma etched. This result emphasized the fundamental differences in the processes of grit-blasting and plasma etching.

ACKNOWLEDGMENTS

REFERENCES

[1] Chin, J. W. and Wightman, J. P., *Composites: Part A* **27A**, 419–428 (1996).

[2] Wenzel, R. N., *Ind. Eng. Chem.* **28**, 988–994 (1936).

[3] Pocius, A. V. and Wenz, R. P., *Proc. 30th Natl. SAMPE Symp.* **30**, 1073–1087 (1985).

[4] Harris, A. F. and Beevers, A., *Int. J. Adhes. Adhes.* **19**, 445–452 (1999).

[5] Kaelble, D. H. and Uy, K. C., *J. Adhes.* **2**, 50–60 (1970).

[6] Smith, T. and Kaelble, D. H., in *Treatise on Adhesives and Adhesion*, R. L. Patrick (Ed.) (Marcel Dekker, New York, 1981), Vol. 5, pp. 139–292.

[7] Carre, A. and Schultz, J., *J. Adhes.* **15**, 151–162 (1983).

[8] Kinloch, A. J., *Adhesion and Adhesives: Science and Technology* (Chapman and Hall, London, 1987), p. 30.

[9] Cherry, B. W., *Polymer Surfaces* (Cambridge University Press, Cambridge, 1981), p. 7.

[10] Page, S. A., Berg, J. C., and Manson, J.-A. E., *J. Adhes. Sci. Technol.* **15**, 153–170 (2001).

[11] Grundke, K., in *Proceedings of the 27th Annual Meeting of the Adhesion Society*, M. Chaudhury (Ed.) (The Adhesion Society, Blacksburg, VA, 2004), pp. 4–6.

[12] Fanconi, B. M., DeVries, K. L., and Smith, R. H., *Polymer* **23**, 1027–1033 (1982).

[13] Peterlin, A., *J. Magnetic Res.* **19**, 83–89 (1975).

[14] Pace, M. D. and Roland, C. M., *Polymer* **32**, 1027–1030 (1991).